Free Radical Biology and Medicine 135 (2019) 102–115

Contents lists available at ScienceDirect

Free Radical Biology and Medicine

journal homepage: www.elsevier.com/locate/freeradbiomed

Original article

# Reduced lifespan of mice lacking catalase correlates with altered lipid metabolism without oxidative damage or premature aging

José Raúl Pérez-Estrada[a], David Hernández-García[a], Francisco Leyva-Castro[a], Javier Ramos-León[a], Osiris Cuevas-Benítez[a], Mauricio Díaz-Muñoz[b], Susana Castro-Obregón[a,1], Ramiro Ramírez-Solís[c], Celina García[a], Luis Covarrubias[a,*]

[a] Instituto de Biotecnología, Universidad Nacional Autónoma de México, Cuernavaca, Mor, Mexico
[b] Instituto de Neurobiología, Universidad Nacional Autónoma de México, Cuernavaca, Mor, Mexico
[c] University of Texas, Health Science Center, San Antonio, TX, USA

ABSTRACT

The relationship between the mechanisms that underlie longevity and aging and the metabolic alterations due to feeding conditions has not been completely defined. In the present work, through the deletion of the gene encoding catalase, hydrogen peroxide ($H_2O_2$) was uncovered as a relevant regulator of longevity and of liver metabolism. Mice lacking catalase ($Cat^{-/-}$) fed ad libitum with a regular diet showed a shorter lifespan than wild type mice, which correlated with reduced body weight, blood glucose levels and liver fat accumulation, but not with increased oxidative damage or consistent premature aging. High fat diet (HFD) and fasting increased oxidative damage in the liver of wild type animals but, unexpectedly, this was not the case for that of $Cat^{-/-}$ mice. Interestingly, although HFD feeding similarly increased the body weight of $Cat^{-/-}$ and wild-type mice, hyperglycemia and liver steatosis did not develop in the former. Fat accumulation due to fasting, on the other hand, was diminished in mice lacking catalase, which correlated with increased risk of death and low ketone body blood levels. Alteration in expression of some metabolic genes in livers of catalase deficient mice was consistent with reduced lipogenesis. Specifically, *Pparγ2* expression up-regulation in response to a HFD and down-regulation upon fasting was lower and higher, respectively, in livers of $Cat^{-/-}$ than of wild type mice, and a marked decay was observed during $Cat^{-/-}$ mice aging. We propose that catalase regulates lipid metabolism in the liver by an evolutionary conserved mechanism that is determinant of lifespan without affecting general oxidative damage.

## 1. Introduction

Aging is the process of organism deterioration that progressively reduces the capacity to keep the general organism homeostasis, increasing the likelihood of death. In contrast, longevity is the length of life from birth to death. Aging is a complex process involving multiple factors going from genetic to environmental and acting at different stages of organism life, including gestation [1]. Since all factors causing aging also reduce lifespan, delaying aging may not extend longevity, but it would extend the healthy life (i.e., health-span; [1,2]).

The good correlation between cellular oxidative damage and aging has been on the basis of the prevalent but still controversial oxidative theory of aging [3]. A premise of this theory is that molecular oxidation causes the cellular damage that accompanies aging. Therefore, lifespan would be determined by the amount of reactive oxygen species (ROS) produced and the capacity to protect against oxidation (e.g., by antioxidants) or the toxic effect of oxidized macromolecules (e.g., by repair or removal; [4]). However, attempts to change the maximal lifespan by increasing or reducing oxidative stress in mice have not resulted in consistent correlations predicted by the oxidative theory, but it does influence the development of a pathology [5]. These observations suggest that under chronic stress, proper function of antioxidant mechanisms could contribute to health-span. Therefore, the role of oxidative stress on aging and health-span is worth of further investigation.

The fact that ROS are unavoidable molecules produced during the process of oxidative phosphorylation as well as of other metabolic reactions such as the β-oxidation of fatty acids implies that metabolic activity would be an intrinsic component of the aging process. Metabolic activity might be a limiting determinant of lifespan as suggested by the key role of the insulin/IGF1 signaling pathway in *Caenorhabditis elegans* (*C. elegans*) and the extension of lifespan promoted by caloric restriction in several species. However, the level at which the control of lifespan due to changes in metabolic activity relies on oxidative damage or ROS-mediated signaling is yet to be determined.

Several antioxidant systems contribute to keep the redox state

* Corresponding author. Av. Universidad 2001, Cuernavaca, Mor, 62210, Mexico.
*E-mail address:* covs@ibt.unam.mx (L. Covarrubias).
[1] Present address: Instituto de Fisiología Celular, Universidad Nacional Autónoma de México, Ciudad de México, México.

https://doi.org/10.1016/j.freeradbiomed.2019.02.016
Received 23 October 2018; Received in revised form 11 February 2019; Accepted 15 February 2019
Available online 25 February 2019
0891-5849/ 

required for normal cell functioning and the prevention of cell damage. For example, controlled balance of cofactors such as $NAD^+$/NADH and $NADP^+$/NADPH is necessary for a broad diversity of reactions, including the ones involved in metabolism and aging [6]. Antioxidant enzymes are expected to contribute to this regulation and, generally, to the control of ROS levels; however, their intracellular localization indicates more specific cellular functions, some directly related with metabolic activity [7]. For example, the mitochondrial localization of superoxide dismutase 2 controls the superoxide produced by the oxidative phosphorylation [8]. On the other hand, the membrane localization of glutathione peroxidase 4 suggests that it protects lipids from peroxidation [9]. In the cytosol, many antioxidant enzymes are present, but the glutathione peroxidase 1 (GPX1) appears to be relevant for proper insulin signaling [10]. Catalase is preferentially located in the peroxisome where likely regulates the levels of $H_2O_2$ produced as a by-product of, among other oxidation reactions, the very long chain fatty acid β-oxidation [11–13]. These functions appear to be irrelevant during mammalian embryogenesis, but the abnormal phenotypes observed in the absence of some of them suggest a function during adult life [14–17].

The liver can be considered a metabolic center where signals from the nervous system and peripheral organs (e.g., pancreas, adipose tissue) converge to maintain the homeostasis of many metabolites required for the well-functioning of cells and organs. In particular, lipid metabolism in hepatocytes is fundamental for the maintenance of systemic energy homeostasis, such that under fed condition insulin promotes lipogenesis and lipoprotein secretion, whereas under fasting, fatty acid oxidation increases eventually producing ketone bodies, an essential energetic resource when glucose is depleted. These processes are critically altered in obesity resulting in accumulation of fat in the liver, a condition that often correlates with the hyperglycemia and insulin resistance that typically characterize type 2 diabetes [18]. Hepatocytes are rich in peroxisomes where catalase is the main protein component, though has also been detected in the cytosol and mitochondria [11,19]. Therefore, it is expected that catalase perform a key antioxidant role in hepatocytes, especially during active fatty acid oxidation.

The catalase of mammals is a homotetrameric enzyme that contains a heme moiety in the active site of each subunit [11]. Mammals have a single gene encoding catalase or homologous enzymes. The catalytic reaction of catalase uses two $H_2O_2$ molecules, the only natural substrate known, to oxidize iron in the heme and release water and oxygen. Catalase activity is among the highest known to be able of degrading $H_2O_2$ in a wide range of concentrations [11]. In the present work, we found that mice lacking catalase have a shorter lifespan than wild type mice and reduced fat accumulation, without an evident increase in oxidative damage. Therefore, we explored the role of catalase in liver under conditions that promote degradation of fatty acids in the liver, a high fat diet and fasting. Our data support a relevant role of peroxisomal $H_2O_2$ in the regulation of lipid metabolism in the liver, a process that could significantly influence lifespan by an evolutionary conserved mechanism.

## 2. Material and methods

### 2.1. Cat null allele generation

The null mutation in the gene encoding catalase (*Cat*) was generated in embryonic stem (ES) cells (AB2.2 line) by standard gene targeting procedures. The 5'- (3.5 kb) and the 3'- (3.3 kb) arms specific for the *Cat* genomic region were inserted in the pPGKNeoloxPA vector containing the $Neo^r$ gene under the control of the PGK promoter flanked by loxP sequences (Fig. S1A). Because of homologous recombination, a 6.2 kb region, containing exons 4–6 and a fragment of 7, was deleted (Figs. S1A and B). The chimeric mice, resulting after blastocyst ES cell injection, were backcrossed with mice of the C57BL/6NJ strain obtained from Jackson Laboratories for more than 10 generations giving rise to the heterozygous $Cat^{+/-}$ line used in the present work. Heterozygous $Cat^{+/-}$ mice were intercrossed to produce mice with $Cat^{+/+}$, $Cat^{+/-}$ and $Cat^{-/-}$ genotype and, in some cases, $Cat^{-/-}$ mice were also produced by incrosses. Mice were genotyped by PCR with specific primers for the wild-type (forward TTGTTACCGCTTTCCTAAACTCC; reverse: TGACTTCCTTGGTCAGATCAAATG) and mutant alleles (forward TGTC ATTCTATTCTGGGGGG; reverse: GGACGACACTTATGAAGCAATC).

### 2.2. Animal protocols

The mice were maintained in plastic cages within a pathogen-free animal facility with humidity-monitored rooms and a 12-h light/dark cycle. Male mice were used for all experiments and were euthanized by cervical dislocation and collected tissues and blood samples stored at −70 °C. Survival along aging was determined in cohorts consisting of 28, 30 and 31 male mice with the $Cat^{+/+}$, $Cat^{+/-}$ and $Cat^{-/-}$ genotypes, respectively, which were maintained in cages with 2–3 individuals, fed with regular chow ad libitum, had free access to water and received standard animal care. The exact birth and death date were recorded, and mice that developed acute skin ulcers, typical of C57BL/6NJ strain, were euthanized and not considered for the survival analysis; relevant to mention is that emergence of skin ulcers did not correlate with the *Cat* genotype (14/28 $Cat^{+/+}$, 11/30 $Cat^{+/-}$ and 14/31 $Cat^{-/-}$) but it did correlate with age (2/89 of 2–9 months, 19/79 of 10–17 months and 18/51 of 18–25 months). Ambulatory and fine activity of individual 12- or 24-month-old (mo) mice $Cat^{+/+}$ or $Cat^{-/-}$ was determined with the Photobeam Activity System (San Diego Instruments Inc, San Diego, CA, USA) and the data analyzed with the PAS Home Cage software (San Diego Instruments Inc, San Diego, CA, USA). Briefly, the activity chamber (11.75" (W) x 18.75" (L)) records the number of times the mouse crosses a photobeam grid oriented on an x and y axis; consecutive photobeam breaks occurring in adjacent photobeams were scored as an ambulatory movement while breaks occurring at same photobeam were scored as fine activity. Cumulative ambulatory and fine activity counts were recorded every 5 min for 24 h (7:00–7:00 daytime); the total activity was the sum of ambulatory and fine activity. Groups of at least 3 mice with the $Cat^{+/+}$ and $Cat^{-/-}$ genotype were collected for each diet or feeding condition. High fat diet (HFD; 60% calories from fat; D12492, Diets Research, New Brunswick, NJ, USA) feeding was initiated, either immediately after winning (i.e., at 21 days of age) and continued for 6 months, or at 3 months of age and continued for 2 or 12 weeks. HFD-control low fat diet for these experiments was the one recommended by the provider (10% calories from fat; D1245B, Diets Research, New Brunswick, NJ, USA). For starvation protocols, 3-mo male mice with a defined *Cat* genotype were collected, fed with a standard diet (1218SX, Envigo, Indianapolis, IN, USA) and food removed at 7:00 daytime and animals sacrificed 24 or 48 h later; in some cases, refeeding was allowed for 12 h starting at 7:00 daytime. Newborn mice with the genotype required for starvation experiments were produced by timed matings of homozygous mice with the desired genotype ($Cat^{+/+}$ *or* $Cat^{-/-}$); at 19 days post coitum a cesarean was performed on pregnant mice. Newly delivered mice were kept in a humidified chamber at 37 °C and continuously monitored to determine survival. Another group of pregnant mice gave birth naturally, and 12 h later pups were transferred to the humidified chamber to follow survival. For the capture of X-Ray images, mice were anesthetized with intranasal 1% isoflurane (Sofloran Vet, PiSA Agropecuaria, Guadalajada, JAL, México) and images captured in a 15 $cm^2$ view field, aperture f/stop of 2.8 and an acquisition time of 5 s with a 0.4 mm filter using the Multimodal Animal Rotation System (MARS) in the In-vivo Xtreme instrument (Bruker, Germany). The AKT activation by insulin was performed in 2-mo mice fed with the standard diet; mice were fasted for 12 h before ip injection of insulin (3 U/kg) or of a saline solution and euthanized 30 min later. All animal procedures described were approved by the Bioethical Committee of our Institute and

rigorously meet international standards.

### 2.3. Blood and serum analysis

Blood was collected from the tail or by cardiac puncture after sacrifice. To obtain serum, blood was incubated for 2 h at room temperature and centrifuged at 2000 g for 10 min; the supernatant recovered was stored at −70 °C until used. Levels of glucose and ketone bodies were determined with the Ascencia Countour glucometer (Bayer, Japan) or the FreeStyle ketone/glucometer (Abbot, Maidenhead, UK), respectively. Insulin was measured with the Ultra-Sensitive Mouse Insulin ELISA kit (Crystal Chem, Downers Grove, IL, USA). Triglycerides and cholesterol in serum were determined using the Triglycerides reagent (BioSystem, Costa Brava, Barcelona, Spain) or the Cholesterol reagent (BioSystem, Costa Brava, Barcelona, Spain) following the manufacturer's instruction. For the glucose tolerance test, glucose (2 mg/kg) was intraperitoneally (ip) injected after a 12 h starvation period and blood glucose concentration immediately measured (time "0") and then at 15, 30, 60 and 120 min after injection. For the insulin tolerance test, 4 h-starved mice were ip injected with a recombinant human insulin (Gibco, Invitrogene, CarlsBad, CA, USA) and blood glucose concentration immediately measured (time "0") and then at 15, 30, 60 and 120 min after injection.

### 2.4. Quantification of total hepatic cholesterol, triglycerides and glycogen

Lipids of liver were extracted by homogenization of 50 mg of tissue in 1 mL of PBS, followed by the addition of 4 ml of Folch reactive (chloroform/methanol 2:1). After vortexing, the suspension was centrifuged at 3000 g for 10 min, and the organic phase transferred to a glass vial for evaporation to dryness at 37 °C overnight. The precipitate was resuspended in 500 µl of 1% sodium deoxycholate solution, and triglycerides and cholesterol concentration determined using the Triglycerides reagent (BioSystem, Costa Brava, Barcelona, Spain) or the Cholesterol reagent (BioSystem, Costa Brava, Barcelona, Spain) following the manufacturer's instruction. For hepatic glycogen content, 40–100-mg of tissue were homogenized in 100 µl of 30% KOH at 100 °C for 30 min. The homogenates were cooled to room temperature and then 100 µl of 20% $Na_2SO_4$ followed by 1 ml ethanol were added. The mixture was left at −20 °C for 6 h and then centrifugated at 3000 g for 10 min; after removal of the supernatant, the pellet was resuspended in 500 µl of 0.2 M sodium acetate buffer pH 4.8 and incubated with 5 units of amyloglucosidase (Sigma-Adrich, Saint Louis, MO, USA) for 8 h at 55 °C. Finally, glucose concentration was measured using the Glucose reagent (BioSystem, Costa Brava, Barcelona, Spain); the data were expressed as nmol equivalents of glucose/g liver.

### 2.5. Determination of conjugated dienes and catalase activity

Livers were homogenized in PBS and total amount of protein recovered determined with the Bradford reagent (Bio-Rad, Hercules, CA, USA) for each resulting sample. Conjugated dienes were determined in lipids extracted as referred above and using previously described procedures [20]. The catalase activity was determined in whole liver homogenates by two methods: (a) in-gel activity, detected by the absence of the Prussian blue precipitate in non-denaturing gels embedded first with $H_2O_2$ and then with a potassium ferrocyanide/ferric chloride solution, or (b) by spectrophotometrically determining the decline in concentration of $H_2O_2$ substrate with time. Both methods were performed following the protocol described by Weydert and Cullen [21].

### 2.6. Histological analysis

Liver tissue samples were fixed with 4% paraformaldehyde overnight and embedded in paraffin wax or in Tissue-Tek (Sakura Finetek, Torrance, CA, USA) for microtome (RM2145, Leica, Nussloch, Germany) or freezing Cryostate sections (CM1850, Leica, Nussloch, Germany), respectively. Paraffin-embedded liver slices were stained with a hematoxylin-eosin cocktail (Sigma-Adrich, Saint Louis, MO, USA) following the manufacturer's instructions. Slices from frozen tissues were stained with red-oil and counterstained with hematoxylin (Sigma-Adrich, Saint Louis, MO, USA), or stained for β-galactosidase activity at pH 6 using the Beta-Galactosidase Tissue Stain Base Solution (Merk-Millipore, Darmstadt, Germany) and counterstained with eosin (Sigma-Adrich, Saint Louis, MO, USA) following the manufacturer's instructions. Similar procedure was followed for hematoxylin-eosin staining of adipose tissue slices but Bouin's fixing solution (Sigma-Adrich, Saint Louis, MO, USA) was used. Bright-field images were acquired using the Olympus BX51 microscope and a C-5050 camera (Olympus, Tokyo, Japan). β-gal-eosin images were quantified using the Image J software (version 2.0.0). Briefly, H&E color deconvolution was applied to each image and the layer corresponding to 'hematoxylin" was selected and converted to a 8-bit format before establishing a threshold. After that, the analysis of particles was performed to obtain the count of blue spots, the mean average of spot size and the total stained area; three images per liver were analyzed.

### 2.7. Immunoblotting

Liver tissue lysates (35 µg protein) prepared in RIPA lysis buffer (50 mM Tris pH7.5, 150 mM NaCl, 1% Triton X-100, 0.5% sodium deoxycholate, 0.1% SDS with protease and phosphatase inhibitors) were separated by electrophoresis on 10% SDS-PAGE gels and transferred to Immobilon-FL membranes (Merk-Millipore, Darmstadt, Germany). The blots were blocked with the Odyssey blocking buffer (LI-COR Biosciences, Lincoln, NE, USA) at room temperature for 1 h and then incubated overnight with the primary antibodies obtained from Cell Signaling (Cell Signaling Technology, Danvers, MA, USA): anti-AMPK (#2532, 1:2000 dilution), anti-pAMPK (#2535, 1:1000 dilution), anti-tubulin (#3873, 1:7000 dilution), anti-AKT (#9272, 1:1000 dilution), anti-pAKT (#2965, 1:1000 dilution), anti-SQSTM1/p62 (#23214, 1:1000 dilution) anti-LC3A/B (#4599, 1:100 dilution). After washing 3 times for 5 min each in a Tris-buffered saline-Tween 20 (0.1%, vol:vol) solution, the membranes were incubated with a goat anti-rabbit IgG or anti-mouse IgG secondary antibodies coupled to infrared fluorophores (emission at 689 or 778 nm; LI-COR Biosciences, Lincoin, NE, USA) at room temperature for 1 h. After washing, the protein bands were visualized in the Odyssey Classic Imaging System (LI-COR Biosciences, Lincoin, NE, USA). Twenty percent SDS-PAGE was used only for the detection of LC3 using liver lysates prepared with RIPA containing 1% SDS. Protein carbonylation was determined using the OxyBlot Oxidation Detection Kit (Merk-Millipore, Darmstadt, Germany). Briefly, carbonyls in proteins were derivatized into 2,4-dinitrophenyhydrazone (DNP-hydrazone) and then processed for western-blot; oxidized proteins were detected with an anti-DNP antibody and visualized in the Odyssey Classic Imaging System (LI-COR Biosciences, Lincoin, NE, USA). Protein bands were quantified by densitometry using the ImageJ software (version 2.0.0).

### 2.8. Gene expression analysis

Total liver RNA was obtained using the RiboEx total RNA isolation solution (GeneAll Biotecnology, Seoul, Korea) following the manufacturer's instructions. This RNA was used as template to synthesize cDNA with the HyperScrip reverse transcriptase (GeneAll Biotecnology, Seoul, Korea) using random hexamers as primers (Invitrogen, US). The quantitative PCR (qPCR) reaction was performed with the SYBR Green mix (KAPA Biosystems, Cape Town, South Africa) in the Rotor-Gene Q thermocycler (Qiagene, Germantown, MD, USA). The sequence of specific oligonucleotides were taken from either reports of others or designed by us using the PrimerBlast3 (see Table S1 for details). In some cases, equal amounts of cDNA from at least 3 individuals were

mixed before qPCR. The relative gene expression level was estimated by the ΔΔCT method, using *Rplp0* expression as an internal control and the indicated mouse group as experimental control.

### 2.9. Statistical analysis

All statistical analyses were done with the Prism software version 5.0b (La Jolla, CA, US) using the Long-Rank test for survival and the two-way variance analysis followed by the Bonferroni test for the other rest of experiments; minimal significance considered was 0.05 (*0.05, **0.01, ***0.001) with a "n" minimal value of 3. All graphs shown are the media ± standard deviation.

## 3. Results

### 3.1. Catalase gene (Cat) inactivation causes premature death without signs of increased oxidative damage or general advanced aging

The *Cat* gene is abundantly expressed in early mouse embryos (Figs. S1C and D) and in several adult organs and tissues like liver, kidney and spleen (Fig. S1E). To determine the function of catalase during embryogenesis and in adult life, we generated a null *Cat* allele by deleting a region (exons 4–6) encoding an essential catalase domain in embryonic stem cells (Figs. S1A and B). Mice homozygous for this null allele ($Cat^{-/-}$) did not show catalase activity (Fig. S1E) supporting that, at least in the tissues tested, there is no other homologous gene that encodes an enzyme with a similar activity. $Cat^{-/-}$ mice were viable, born with the expected mendelian ratio but, interestingly, showed a decreased lifespan in comparison with $Cat^{+/+}$ and $Cat^{+/-}$ mice (Fig. 1A). Twelve-months old (mo) or 24-mo mice lacking catalase did not show evident signs of more advanced aging than wild type such as higher density of gray hairs, alopecia or reduced motor activity (Fig. 1B and C). Accordingly, the increasing lipid peroxidation observed along the first 10 months of life in several organs was similar between wild type and mice lacking catalase (Fig. 1D) or even lower in livers of 24-mo $Cat^{-/-}$ mice (see below). However, X-ray images revealed kyphosis (hunchback) in $Cat^{-/-}$ mice since 12-months of age, a phenotype that was more pronounced in 24-mo mice (Fig. 1E). Despite this latter evident phenotype associated with advanced aging, no other data indicated premature aging as the cause of death. Relevant to mention is that, although initial increase in weight with age was similar, mutant 24-mo mice were slimmer than wild type mice (Fig. 1E and F), despite the fact that there were no signs of any sickness (e.g., piloerection, presence of tumors) and that, in general, animals were active near death (Fig. 1C). In addition, the characteristic hyperglycemia of old mice did not develop in mice lacking catalase (Fig. 1G), though insulin levels increased with age as in wild-type mice (Fig. 1H). Circulating levels of triglycerides, cholesterol and ketone bodies were as in wild-type mice (Fig. 1I–K).

Since a distinctive characteristic of liver is the presence of high catalase activity, this organ of $Cat^{-/-}$ mice would be expected to show detectable cellular and molecular alterations. Increased lipid oxidative damage occurred in the liver of wild type mice with aging but, unexpectedly, this was not found in the liver of $Cat^{-/-}$ mice, which showed even reduced lipid oxidative damage at the age of 24 months (Fig. 2A) and there was no difference in liver protein oxidation between $Cat^{-/-}$ and wild type mice at 12- and 24-months of age (Fig. 2B). No compensatory activity of peroxidases (Fig. S1E) or an antioxidant response were detected in the liver of mice lacking catalase (Fig. S1F). In contrast, staining for β-galactosidase at pH6, a commonly used indicator of cellular senescence within a tissue, emerged in livers of $Cat^{-/-}$ at earlier age and spots were in higher number and covered a larger area than in those of $Cat^{+/+}$ mice (Fig. 2C). However, the association of this difference with cellular senescence could not be established because, as expected, livers of wild type and of $Cat^{-/-}$ mice showed similarly increasing levels with age in *p16*, *p21* and *p53* expression (Fig. 2D). Interestingly, liver fat accumulation with aging, as revealed by red oil staining, in *Cat* deficient mice was lower than in wild type mice (Fig. 2E), and particularly coincided with triglycerides and cholesterol levels detected in livers of 24-mo mice (Fig. 2F and G). No difference in liver glycogen content was found between wild-type and $Cat^{-/-}$ mice at any age tested (Fig. 2H). Therefore, the liver of $Cat^{-/-}$ mice do not show consistent characteristic of premature aging.

### 3.2. The lack of catalase prevents from oxidative damage and fat accumulation in the liver in response to feeding with a HFD

Oxidative damage or premature aging was not obviously related with the reduction in lifespan of catalase deficient mice. Instead, the slim appearance of old mutant mice together with their relatively low levels of blood glucose and of accumulated liver fat suggested that metabolic alterations are behind premature death. In agreement with the participation of catalase in fat metabolism in the liver (Fig. 3A), wild type mice fed with a HFD markedly decreased catalase activity (Fig. 3B) with a corresponding increment in lipid peroxidation (Fig. 3C). Paradoxically, the liver of $Cat^{-/-}$ mice did not show the increment in lipid peroxidation in response to HFD, though increased levels were detected when these mice were fed with the HFD-control diet (Fig. 3C). The contrasting difference between this latter observation and the one shown above (Fig. 2A) could be due to the diet composition; particularly, the HFD-control has 2/3 of the amount of polyunsaturated fat in standard chow, and the caloric supply of fat and carbohydrates in HFD-control is lower and higher, respectively, than those in standard chow (see more details in Table S2). These data together indicate that the absence of catalase prevents from the rise in ROS levels in association with a HFD.

An evident sign of the effect on fat metabolism due to a long-term HFD feeding is the accumulation of fat in liver, pathology known as hepatic steatosis. In agreement with the absence of evident abnormalities due to the lack of catalase, $Cat^{-/-}$ and $Cat^{+/+}$ mice fed with a HFD-control diet did not show body weight or feeding behavior differences during adult life (Fig. 3D, Fig. S2A). In addition, the pattern of increase in body weight and feeding behavior under a HFD was also similar for mice with either genotype (Fig. 3D, Fig. S2A). However, mice lacking catalase showed attenuated hepatic steatosis (Fig. 3E) and decreased triglycerides and cholesterol content in liver in comparison with wild type mice after 3 months feeding with a HFD (Fig. 3F and G), though an alteration in liver weight associated with the lack of catalase was not evident (Fig. S2B). The absence of catalase did not seem to affect adipocyte size or level of macrophage infiltration in the white tissue of epididymus (Fig. S2C), common in obese mice. Brown subcutaneous interscapular or white epidydimal fat tissue weight did not change in association with the levels of catalase (Figs. S2D and E) and evident accumulation of white adipose tissue was noted in all mice fed with a HFD (Fig. S2F). Therefore, HFD, instead of increasing oxidative damage in livers of $Cat^{-/-}$ mice, causes changes in the lipid metabolic pathways that generate steatosis (see below).

### 3.3. Mice lacking catalase fed with HFD do not develop hyperglycemia and glucose intolerance

It is widely known that mice fed for a long term with a HFD causes obesity and, consequently, hyperglycemia, glucose intolerance and insulin resistance. Recent data have also shown that these alterations in glycemia are strongly associated with liver steatosis [22]. The glycemia determined at 12-weeks after feeding with a HFD showed that $Cat^{-/-}$ mice did not develop the typical hyperglycemia observed in wild type mice, and glucose levels remained in a similar range as mice fed with the HFD-control diet (Fig. 3H). In agreement with this observation, the increase in insulin, typical in response to HFD feeding, was not observed in $Cat^{-/-}$ mice (Fig. 3I) and levels were similar to those observed in mice fed with the standard diet (Fig. 1H). Accordingly, and in

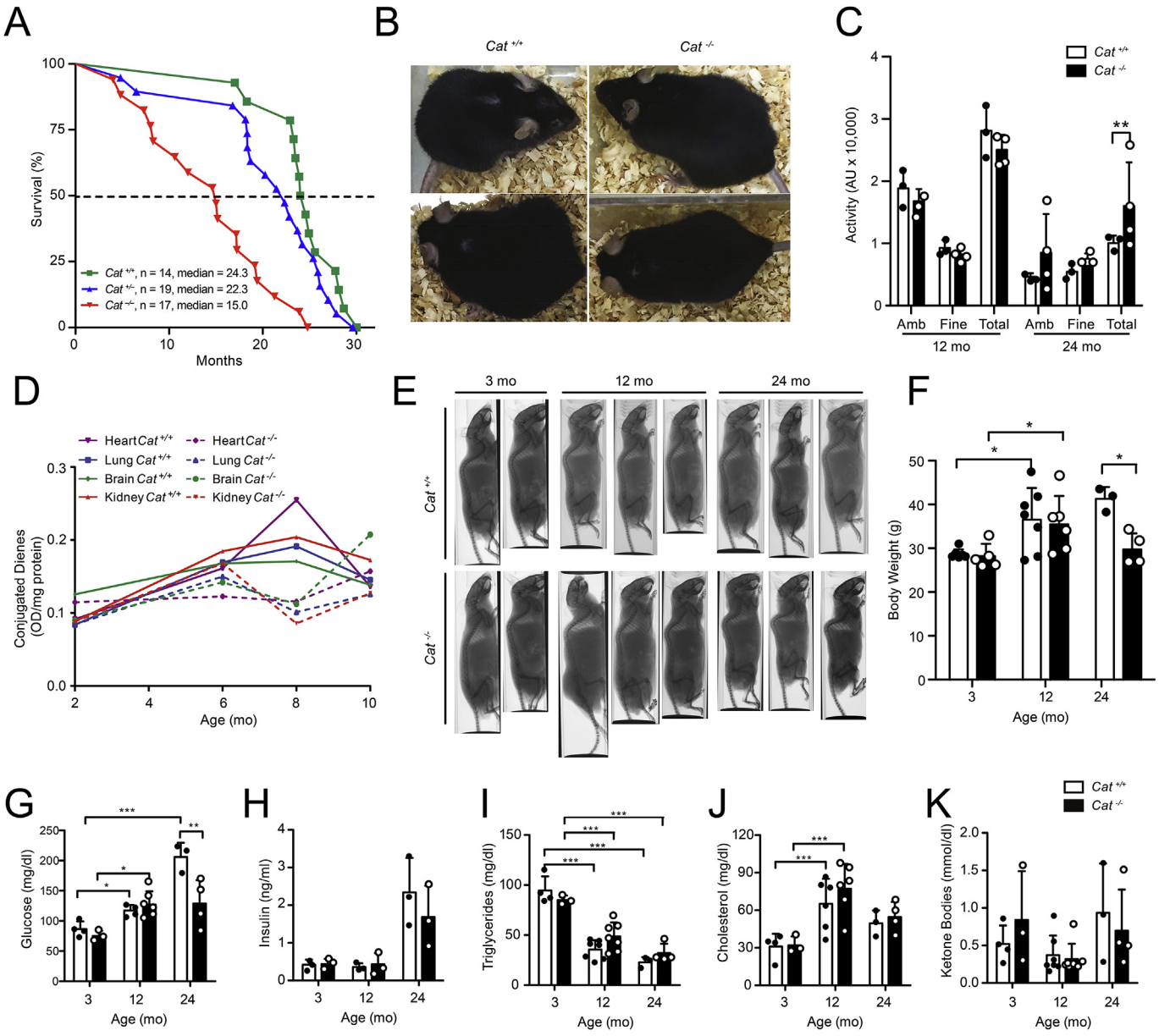


**Fig. 1. Lifespan and aging parameters of mice with ($Cat^{+/+}$) or without ($Cat^{-/-}$) catalase.** (A) Lifespan of $Cat^{+/+}$, $Cat^{+/-}$ and $Cat^{-/-}$ mice. Survival difference between $Cat^{+/+}$ and $Cat^{-/-}$ mice is statistically significant ($p < 0.0001$, Long-Rank test) and also between $Cat^{+/-}$ and $Cat^{-/-}$ mice ($p < 0.0012$) but not between $Cat^{+/+}$ and $Cat^{\pm}$ mice ($p < 0.1773$). (B) Representative photographs of 18-mo $Cat^{+/+}$ and $Cat^{-/-}$ mice. (C) Motor ambulatory (Amb), Fine (F) and Total (T), activity of 12- and 24-mo $Cat^{+/+}$ and $Cat^{-/-}$ mice. (D) Lipid oxidation, as estimated by the amount conjugated dienes, in whole extracts of heart, lung, brain and kidney of 2–10-mo mice. (E, F) X-ray images (E) and body weight (F) of 3-, 12- and 24-mo mice. (G–K) Glucose (G), insulin (H), triglycerides (I), cholesterol (J) and ketone bodies (K) levels in serum of 3-, 12- and 24-mo mice. Note that the lack of catalase in mice did not correlate with increased oxidative damage in several organs or consistent premature aging, but lower blood glucose levels and body weight were observed in mice lacking catalase. All values shown are the mean ± SD; n = 3–9. $*p < 0.05$, $**p < 0.01$ and $***p < 0.001$ (two-way variance analyses).

contrast with wild type animals, the $Cat^{-/-}$ mice fed with a HFD responded to an elevation in blood glucose concentration in a similar manner as wild type or mutant mice fed with the HFD-control diet (Fig. 3J). Interestingly, the response to high insulin dose of $Cat^{-/-}$ mice fed with a HFD-control diet was as of wild type mice, whereas when feeding was with a HFD, the initial response was similar among mice with any *Cat* genotype but recovery towards normal glucose levels was notoriously more rapid in animals lacking catalase (Fig. 3K). This phenomenon does not seem to be related to alterations in insulin signaling, since basal and insulin-stimulated levels of AKT phosphorylation were not modified by the absence of catalase (Fig. 3L,M; see also data below); nonetheless, increased gluconeogenesis could be responsible of the rapid recovery in glucose levels after the decline induced by insulin. These data are in agreement with the reduced accumulation of fat in the liver of $Cat^{-/-}$ mice that, consequently, prevents from losing the homeostatic control of glucose under a HFD.

### 3.4. The lack of catalase decreases the viability of mice under fasting conditions

Another condition that causes significant changes in lipid metabolism is fasting. Shortly after food deprivation, free fatty acids are brought from the adipose tissue to the liver causing the accumulation of fat in the form of lipid droplets [23]. The immediate source of glucose under food deprivation is glycogen but later fatty acids are directed to produce ketone bodies which are used as a major energetic source when

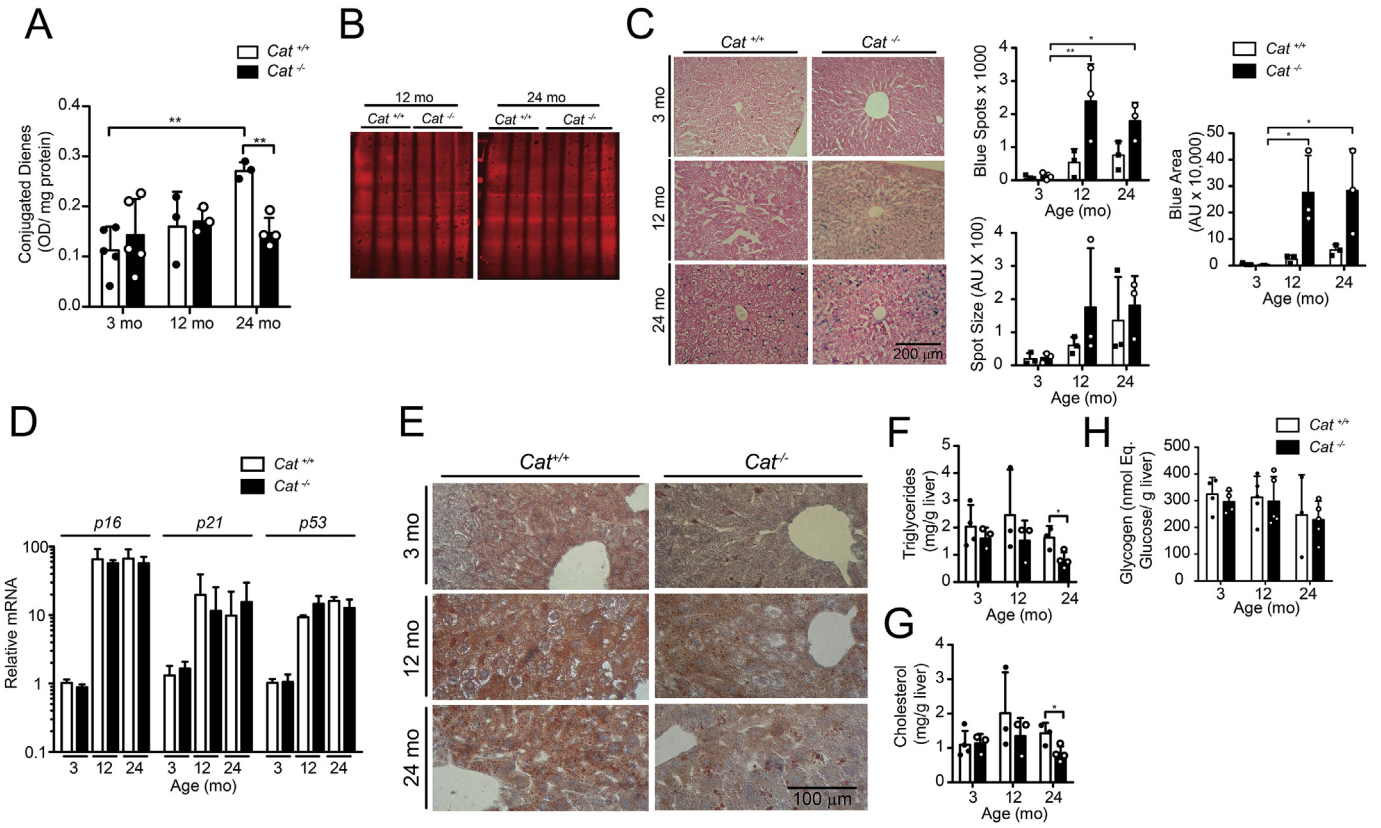


**Fig. 2. Oxidative damage, cellular senescence and fat accumulation in livers of aging mice with ($Cat^{+/+}$) and without ($Cat^{-/-}$) catalase.** Determinations were done in 3-, 12- and 24-mo mice. (A) Lipid oxidation in liver as determined by the amount of conjugated dienes. (B) Protein oxidation (immunoreactivity against DNP) in livers of 12- and 24-mo mice; no signal was detected before carbonyl derivatization into DNP-hydrazone. (C) Representative images of β-galactosidase stained liver sections. Level of staining was determined by counting the number of blue dots and estimating the area covered by them in representative sections of livers. (D) Expression of the senescence-related genes indicated determined by qRT-PCR. (E) Representative images of red-oil stained liver sections. (F, G, H) Triglycerides (E), cholesterol (F) and glycogen (H) content in liver. Note that the levels of oxidative damage correlated better with fat accumulation than with markers of cellular senescence. All values shown are the mean ± SD; n = 3–5. $*p < 0.05$, $**p < 0.01$ and $***p < 0.001$ (two-way variance analyses).

glucose supply is short [24].

In wild type mice, catalase activity and expression of its gene decreased during fasting, and their recovery was still incomplete 12 h after refeeding (Fig. 4A, Fig. S3A). In agreement with the decrease in catalase activity, the lipoperoxidation increased (Fig. 4B), suggesting that catalase normally participates in the metabolic changes associated with this condition. Weight loss throughout 48 h fasting and the corresponding weight gain after refeeding was not markedly altered in $Cat^{-/-}$ mice in comparison with wild type mice (Fig. 4C). Also, the lack of catalase did not cause significant differences in the early elevation and abrupt decline of blood glucose (Fig. S3B), and the expected increase in ketone bodies (Fig. 4D). Blood levels of cholesterol and triglycerides, and the liver glycogen content after 24 h and 48 h fasting in $Cat^{-/-}$ was as in wild type mice (Fig. S3 C-E). In contrast, the characteristic fat accumulation (Fig. 4E–G) and increased lipoperoxidation at 48 h (Fig. 4B) in the liver of wild type mice was reduced in $Cat^{-/-}$ mice. In agreement with a rise in protein recycling due to fasting, expression of autophagy/lysosome genes (*Atg5*, *Atg7*, *LC3B*, *p62*, *Lamp2*) and a gene associated with activation of ubiquitin-proteosome (*Atrogin-1*) increased in livers of $Cat^{-/-}$ and $Cat^{+/+}$ mice after 24 h of fasting (Fig. S3F). However, although the levels of p62 decreased similarly in livers of mice of both genotypes, the levels of LC3II, the autophagosome-associated form of LC3I that reflects autophagy activity [25], were moderately higher in livers of mice lacking catalase (Fig. S3G). Therefore, as in the HFD feeding condition, reduced fat accumulation accompanied by a lower oxidative damage was the major consequence of fasting in livers of mice lacking catalase.

The metabolic alterations described above were apparently no life-threatening for $Cat^{-/-}$ mice. However, it was common to find that some catalase deficient mice at 48 h of starvation, just before sacrifice, got still, a characteristic that correlated with an evident necrotic small bowel and was considered a sign of imminent death (Fig. 4H). Interestingly, these dying $Cat^{-/-}$ mice also showed an abrupt exhaust of ketone bodies (Fig. 4D, red dots). No wild type mice showed any of these characteristics at this time of fasting. Since it is well-known that the viability of starved newborn mice strongly depends on their capacity to use the energetic resources available (e.g., glycogen and ketone bodies; [26,27]), we tested the viability of newborn $Cat^{-/-}$ mice. Interestingly, the survival of $Cat^{-/-}$ newborn mice was reduced in comparison with wild type newborn mice under acute (Fig. 4I) or moderate starvation (Fig. 4J). Serum ketone bodies sharply decreased in $Cat^{-/-}$ mice after 6-h fasting, whereas reduction in $Cat^{+/+}$ mice was noted until 12-h fasting (Fig. 4K). Likewise, glucose levels decreased earlier in $Cat^{-/-}$ than in wild type (2-h vs. 6-h fasting; Fig. 4L), though this effect did not correlate with glycogen content (Fig. S3H). No major differences were detected in cholesterol and triglycerides liver content (Figs. S3I and J). Therefore, the depletion of substrates needed for production of ketone bodies might be behind the reduced viability, although the reduction in other energetic resources relevant under these conditions (e.g., amino acids; [28]) should also be considered.

### 3.5. Catalase deficiency reduces lipogenesis and maintains relatively high AMPK activity in the liver

The previous results suggest that the absence of catalase promote metabolic alterations that are detected when mice are subjected to

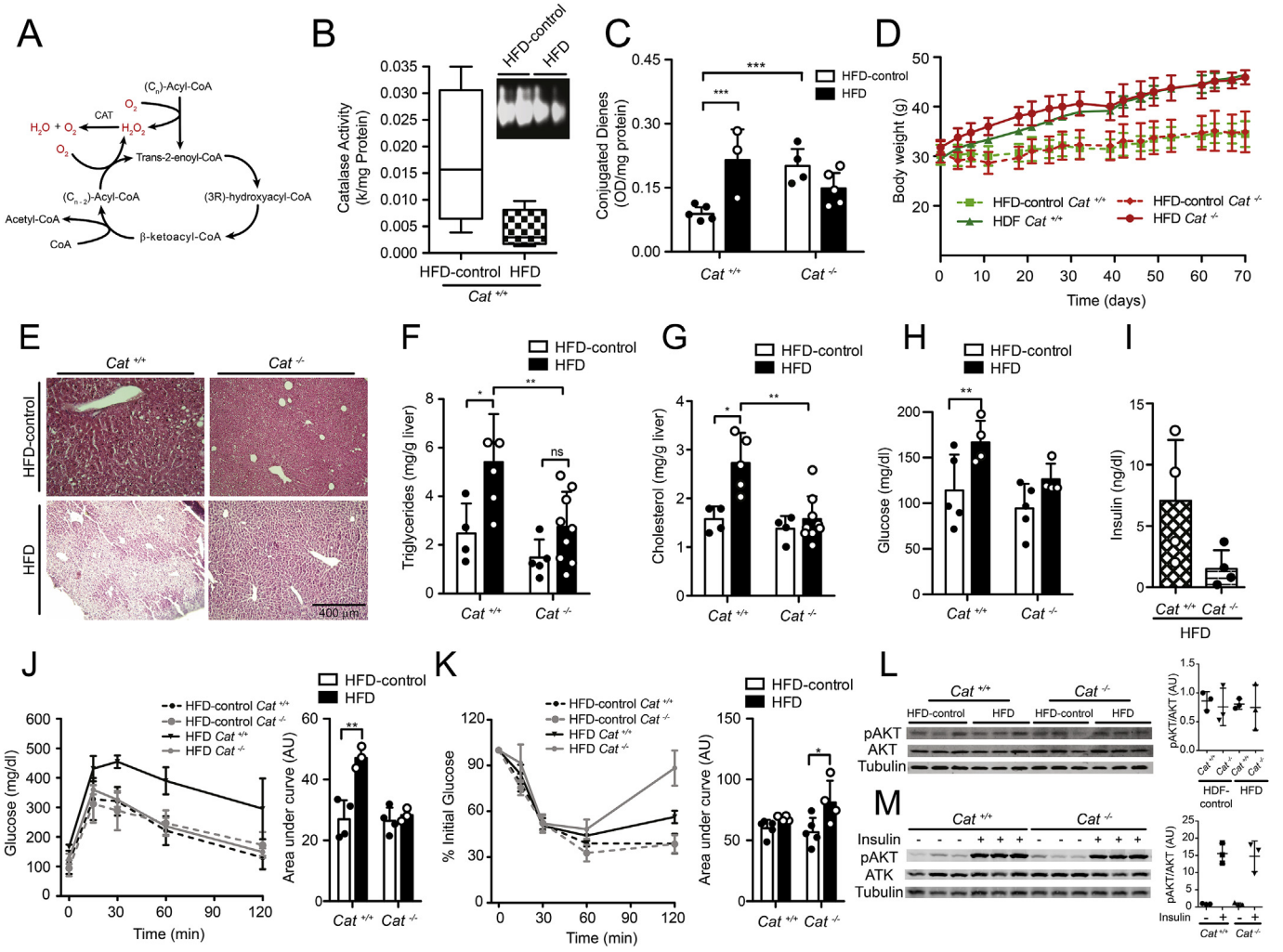


**Fig. 3. Liver oxidative damage and metabolic parameters in mice with (*Cat*$^{+/+}$) and without (*Cat*$^{-/-}$) catalase under a high fat diet.** Determinations were done in samples from mice fed with HFD-control diet or high fat diet (HFD) for 6 months. (A) Schematic representation of $H_2O_2$ production throughout every cycle of peroxisomal fatty acid β-oxidation. (B) Liver catalase activity. Inset shows catalase activity determined by a gel-based assay. (C) Liver oxidative damage, as estimated by the amount of conjugated dienes. (D) Body weight gain. (E) Representative images of hematoxilin-eosin stained liver sections. (F, G) Triglycerides (F) and cholesterol (G) content in liver. (H, I) Glucose (H) and insulin (I) serum levels. (J, K) Glucose levels during the glucose (J) and insulin (K) tolerance tests performed on mice after fed with the diets indicated. Areas under the curve are shown for statistical comparative analyses. (L, M) Liver pAKT and AKT, determined by western-blot, in mice fed with HFD-control and HFD (L) and after insulin infusion to mice fed with standard chow (M). Note that the liver oxidative damage and fat accumulation in response to HFD did not occur in mice lacking catalase, observations that correlated with the apparent increased insulin sensitivity. All values shown are the mean ± SD; n = 3–9. *$p < 0.05$, **$p < 0.01$ and ***$p < 0.001$ (two-way analysis variance).

feeding regimes that affect lipid metabolism. In order to get insights into the metabolic pathways altered in the liver by the lack of catalase, we estimated the expression levels of metabolic genes. In basal conditions (i.e., ad libitum ingestion of standard chow), gene expression showed downregulation of several selected genes (e.g., *Gck, Pparγ2, Spot14, Fasn*) in the liver of *Cat*$^{-/-}$ mice (Fig. S4A). When this comparison was done with liver samples from animals fed with food pellets of different composition (i.e., HFD-control diet; Tables S2–S4), some of the genes tested showed a contrasting expression pattern (*Gck*, *Pck1*, *G6pc*, *Fgf21*, *Cpt1a*) and downregulation of some lipogenic genes was not as evident in livers of mutant mice (e.g., *Spot14, Fasn*; Fig. S4B). This differential gene expression detected is possibly due to the nutrient composition of food pellets provided (Tables S2–S4) that, as described above, also affected the levels of lipid peroxidation.

Under feeding with a HFD for 3 months, mRNA levels of lipogenic genes (*Acc, Fasn*, *Elov6, Scd1* and *mGpat*), included the positive regulators *Pparγ2* and *Spot14*, were lower in livers of *Cat*$^{-/-}$ than of wild type mice (Fig. S4C). The expected expression up-regulation of *Fasn*, *Spot14* and *Pparγ2* was detected since 15 days after HFD feeding in the liver of wild type mice, whereas no or a mild effect was observed in the liver of mice lacking catalase (Fig. 5A); of note was the significant response of the *Pparγ2* gene in livers of wild type mice that, although upregulated in livers of *Cat*$^{-/-}$ mice, the increase in mRNA levels was much lower. Significant difference in the liver expression levels of gluconeogenic genes was not detected when comparing wild type mice with mice lacking catalase fed with a HFD (Fig. 5A). The downregulation of lipogenic gene expression in the liver of *Cat*$^{-/-}$ mice under a HFD is in agreement with the key role of lipogenesis in the generation of hepatic steatosis [22,29].

On the other hand, the mRNA levels of genes associated with catabolism such as *Gck* (encoding the first enzyme in the degradation of glucose), *Acox1* (encoding the first enzyme of the peroxisomal fatty acid β-oxidation pathway) and *Fgf21* (encoding a growth factor released in association with lipolysis) were higher in *Cat*$^{-/-}$ mice after 3 months of HFD feeding (Fig. S4C). Among these genes, only the expression of *Gck* responded to two-weeks HFD feeding (Fig. 5A), showing upregulation in livers of wild type mice as previously reported [30], but this effect was reduced in those of *Cat*$^{-/-}$ mice. These data together suggest

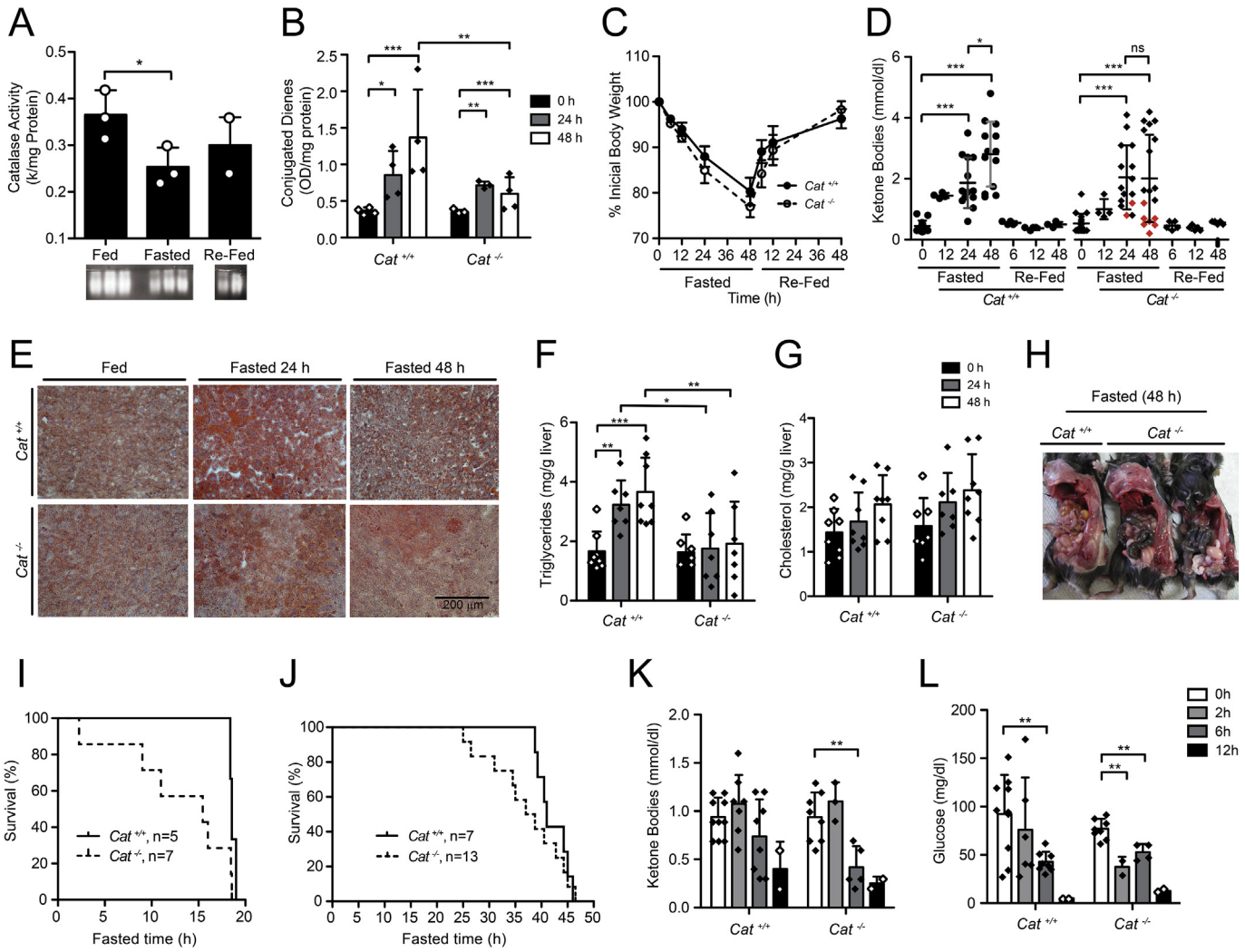


**Fig. 4. Oxidative damage and fat accumulation in livers of mice with (*Cat*$^{+/+}$) and without (*Cat*$^{-/-}$) catalase after fasting.** Adult mice were fasted for up to 48 h and measurements were done at the same daytime (9 AM). (A) Liver catalase activity after 24 h fasting and after refeeding for 12 h. The picture below shows catalase activity determined by a gel-based assay. (B) Liver oxidative damage, as estimated by the amount of conjugated dienes. (C) Percent of body weight loss across 48 h fasting/48 h refeeding. (D) Serum ketone body levels across 48 h fasting/48 h refeeding. Red dots are serum ketone body levels of mice that are about to die (i.e., still and did not respond to touch) at the time of fasting indicated. (E) Representative images of red-oil stained sections from livers of mice, fed or fasted, with the genotype indicated. (F, G) Triglycerides (F) and cholesterol (G) content in livers. (H) Aspect of bowel of mice after 48 h fasting. Note the necrotic aspect of the bowel of fasted mice lacking catalase. (I, J) Survival of fasted (I) or 6 h-fed (J) newborn mice. (K, L) Serum ketone body (K) and glucose (L) levels of newborn mice across fasting. Note that, apparently, reduced fat accumulation and ketone body production is the cause of reduced survival of mice lacking catalase. All values shown are the mean ± SD; n = 3–10. $^{*}p < 0.05$, $^{**}p < 0.01$ and $^{***}p < 0.001$ (two-way analysis variance). (For interpretation of the references to color in this figure legend, the reader is referred to the Web version of this article.)

that the lack of catalase causes a reduction in lipogenesis leading the metabolic balance to favor catabolic activity.

Fasting is a short-term metabolic shift that could reveal the direct metabolic consequence of lacking catalase. The expression of *Pparγ2, Spot14*, *Fasn*, *Scd1* and *Gck* was similarly reduced upon fasting for 24 h, though the recovery to the level before fasting did not occur in all these genes at 12 h after refeeding. In contrast with the downregulation observed in the expression of lipogenic genes and *Gck*, the expression of gluconeogenic (*Pck1*) and catabolism-associated (*Ppara*, *Fgf21*, *Cpt1a*) genes was upregulated upon fasting and downregulated after refeeding (Fig. 5B and C). Despite the expression level of some genes in livers of *Cat*$^{-/-}$ were lower than those of wild type mice, generally the regulatory patterns described above were similar, although it was particularly interesting to note that *Pparγ2* downregulation upon fasting was more pronounced in samples of *Cat*$^{-/-}$ mice (7- vs. 16-fold reduction; Fig. 5B). In newborns, *Gck* in livers of *Cat*$^{-/-}$ mice was expressed at higher levels than in livers of *Cat*$^{+/+}$ mice, and a pronounced downregulation was detected in the former but not in the latter after fasting; the liver expression of other genes tested similarly changed in newborn mice of either genotype in response to fasting (Fig. 5D). The downregulation and upregulation response upon fasting of lipogenic and gluconeogenic genes, respectively, in livers of adult *Cat*$^{-/-}$ mice indicate that the main insulin/glucagon regulatory pathways that control metabolic gene expression are not markedly affected due to the lack of catalase and, thus, reduced lipogenesis and fat accumulation in mice lacking catalase is rather due to an affected central modulator of liver metabolism.

Activation of AMPK by phosphorylation reduces lipogenesis and increases general catabolism [31]. Under HFD-control diet for at least 2 weeks, the liver of mutant mice showed higher levels of activated AMPK than the liver of wild type mice (Fig. 6A), and no change in pAMPK levels could be detected when HFD was provided for as long as 3 months to either *Cat*$^{-/-}$ or *Cat*$^{+/+}$ mice (Fig. 6B). Feeding with the standard chow did not result in consistent higher levels of pAMPK in

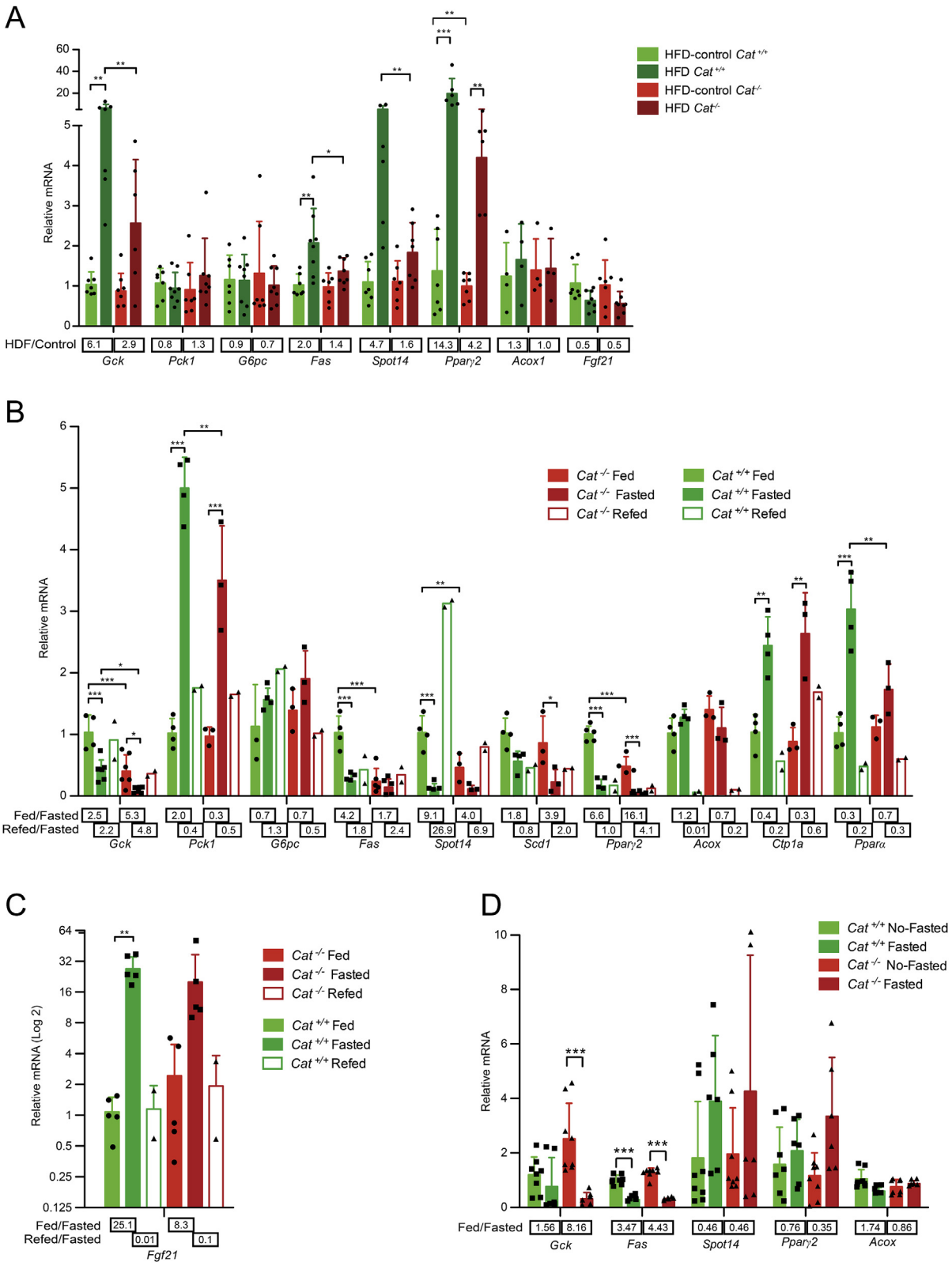


**Fig. 5. Expression of metabolic genes in livers of mice with (*Cat*$^{+/+}$) and without (*Cat*$^{-/-}$) catalase fed with high fat diet or fasted.** Expression levels in the liver of individual mouse either fed with a high fat diet (HFD) for 2 weeks or fasted for 24 h were determined for the genes indicated. (A) Gene expression in livers of mice fed with HFD-control diet or HFD. (B–C) Gene expression in livers of fed, fasted or refed mice. (D) Gene expression in livers of 12 h fasted newborn mice. Numbers within squares are the fold difference between bars above (estimated from the ratio of corresponding averages). Note the reduced up-regulation (upon HFD) or expression levels (before and after fasting) of *Gck* and lipogenic genes. All values shown are the mean ± SD; n = 3–5. *$p < 0.05$, **$p < 0.01$ and ***$p < 0.001$ (two-way analysis variance).

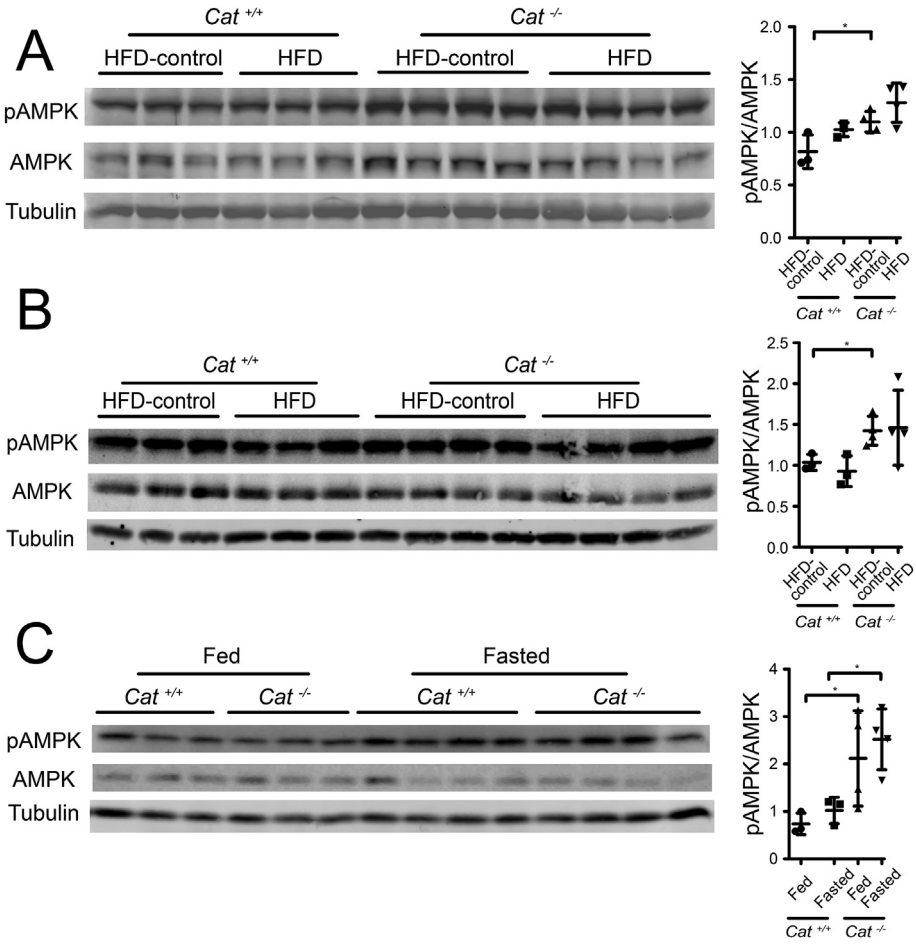


**Fig. 6. Levels of activated AMPK in livers of mice with (*Cat*$^{+/+}$) and without (*Cat*$^{-/-}$) catalase fed with high fat diet or fasted.** AMPK activation in liver was inferred from levels of phosphorylated AMPK (pAMPK) determined by western-blot. Quantification of the pAMPK/AMPK ratio is shown in graphs. (A, B) Activated AMPK in liver of mice fed with HFD-control diet and HFD for 2 weeks (A) or for 3 months (B). (C) Activated AMPK in liver of mice fed or fasted for 24 h. Note a higher level of activated AMPK in livers of mice lacking catalase. All values shown are the mean ± SD; n = 3–4. *$p < 0.05$ (two-way analysis variance).

livers of *Cat*$^{-/-}$ mice in comparison with those of *Cat*$^{+/+}$ mice but, as expected, the proportion of pAMPK increased in response to fasting (Fig. 6C). Therefore, at least in the presence of HFD, higher levels of activated AMPK in livers lacking catalase could contribute to lipogenesis downregulation.

### 3.6. Downregulation of the lipogenic master gene Pparγ2 and the lipolytic gene Fgf21 could contribute to the reduction in lifespan of mice lacking catalase

Short longevity of *Cat*$^{-/-}$ mice could be related to the metabolic alterations described above. Aged mice (12-mo or 24-mo) showed elevated expression levels of gluconeogenic genes in livers of both *Cat*$^{+/+}$ and *Cat*$^{-/-}$ mice in comparison with their corresponding young animals (3 mo; Fig. 7A), which might be expected due to the development of insulin resistance with aging [32]. *Fasn* expression increased with age (3-mo, 12-mo and 24-mo) in both wild type and mice lacking catalase and, although the difference in level of expression remained, was not significant in old animals. Higher levels of pAMPK were particularly notorious in 24-mo mutant mice (Fig. 7B). In previous experiments the pattern of *Fasn* expression positively correlated with that of *Spot14*, however, during aging, *Spot14* expression levels did not change in mice of either *Cat* genotype. Remarkably, while *Pparγ2* expression in liver did not markedly change along wild type mice aging, it was reduced with age in *Cat*$^{-/-}$ mice. Also, the liver of 24-mo mice lacking catalase showed significant lower levels of *Fgf21* expression than the liver of 24-mo wild type mice; low expression levels of *Fgf21* correlated with reduced expression of other catabolic genes such as *Cpt1* and *Acox* (Fig. 7A). In kidney, *Pparγ2* has shown to be a positive transcriptional regulator of *α-Klotho* [33], a gene involved in the control of longevity [34]. In the liver, *β-Klotho* is much more abundant than *α-Klotho* [35] and is the specific co-receptor of Fgf21 [36], therefore, we investigated whether its expression correlated with the one determined for *Pparγ2*. Despite the great difference in *α-* and *β-Klotho* expression level in liver (estimated of more than 100-fold), the expression levels of both *Klotho* genes increased in aged mice (i.e., 12- and 24-mo) regardless of the presence or absence of catalase (Fig. 7C). Autophagy was not notably affected by the absence of catalase along aging (Fig. 7D, Fig. S4D), though a consistent LC3 isoform of slightly higher molecular weight than LC3-II was exclusively present in livers of 12-mo and 24-mo *Cat*$^{-/-}$ mice (Fig. 7D). In summary, low fat accumulation, involving the participation of PPARγ2 activity, and diminished catabolic activity, involving the participation of FGF21 signaling, in the liver could be the cause of the limited lifespan of aged *Cat*$^{-/-}$ mice.

## 4. Discussion

Traditionally, ROS have been considered damaging molecules for the cell but, presently, a variety of studies indicate that ROS play a regulatory role in many cell processes [37,38]. The fact that the activity of many proteins depends on their oxidation state is in agreement with this regulatory role of ROS. Here we propose that $H_2O_2$, rather than

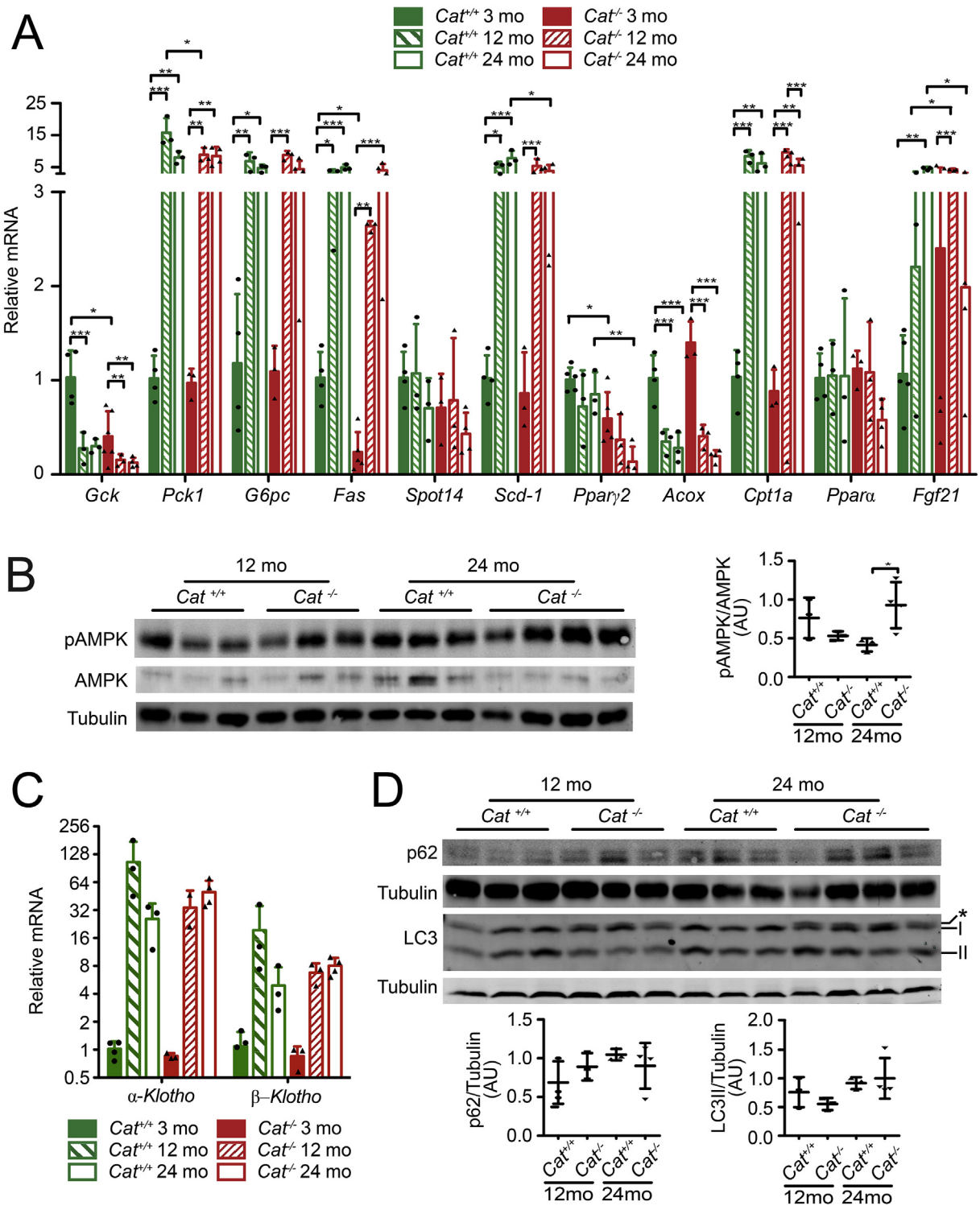


**Fig. 7. Metabolic gene expression and levels of activated AMPK in livers of aging mice with (*Cat*$^{+/+}$) and without (*Cat*$^{-/-}$) catalase.** Determinations were done in livers of 3-, 12- and 24-mo mice. (A) Expression of selected metabolic genes. (B) Levels of activated AMPK (pAMPK). Quantification of the pAMPK/AMPK ratio is shown in graphs. Note the marked up-regulation of gluconeogenic genes in 12- and 24-mo mice of either genotype and the contrasting pattern of *Pparγ2* expression across aging. Also, pAMPK was very abundant in livers of 24-mo mice lacking catalase. (C) Expression of *α-Klotho* and *β-Klotho* genes. (D) Levels of autophagy markers p62 and LC3; asterik in blot photograph points the extra band above LC3-I detected only in livers of mice lacking catalase. All values shown are the mean ± SD; n = 3–4. $p < 0.05$, $^{**}p < 0.01$ and $^{***}p < 0.001$ (two-way analysis variance).

causing a general macromolecular damage, alters metabolism with consequences in the mechanisms that determine longevity. Apparently, the metabolic pathways affected by the lack of catalase are influenced by feeding conditions and additional genetic factors [39,40].

### 4.1. Peroxisome and lipid metabolism

Due to the many oxidase reactions occurring in the peroxisome, this organelle produces a high amount of $H_2O_2$ [12,13]. Accordingly, peroxisomes are also rich in many antioxidants, among which catalase is

the most abundant. $H_2O_2$ could diffuse throughout the peroxisomal membrane passively and the derived ROS (i.e., hydroxyl radical) generally damage cellular macromolecules. However, it is apparent that intraperoxisomal-produced ROS restricts their influence to the redox state of peroxisomes and mitochondria, whereas, peroxisomes are rather resistant to oxidation by ROS produced from different cell compartment including mitochondria [41]. Therefore, the absence of general increased lipid oxidation due to the expected rise in $H_2O_2$ in mice lacking catalase could be due to the restricted oxidation of macromolecules in peroxisomes and mitochondria, whereas the diminished liver oxidative damage caused by a HFD or fasting could be a consequence of the metabolic alterations downstream resulting from specific protein oxidation or changes in the redox balance within these organelles (see below). Hormesis, possibly generated from the moderate increase in ROS in mice lacking catalase, could also contribute to explain the better handling of the rise in ROS under a HFD or fasting, however, up to date we have not detected evidence of a compensatory antioxidant response (Figs. S1E and F), in agreement with other reports [39,42].

The function of peroxisomes in fatty acid metabolism is presently well established [12]. Without disregarding other fundamental functions such as synthesis of ether-phospholipids, biliary acids and essential precursors of cholesterol, one major function of peroxisomes, as mitochondrial β-oxidation efficiency reduces, is a significant contribution to oxidation of long-chain fatty acids and the exclusive oxidation of very long-chain fatty acids [12,13]. Our results indicate that catalase has a relevant function in the regulation of fatty acid metabolism in the liver such that lack of catalase resulted in reduced lipid storage. Under a HFD, liver lipid storage is increased, at least in part, by increased lipogenesis [43]. Lipogenesis upregulation in this condition could derive from AMPK downregulation followed by the rise in SREBP-1c activity due to reduced AMPK-mediated phosphorylation and, consequently, upregulation of lipogenic genes [43]. Contribution of PPARγ2 is particularly relevant in this regard, functioning as a positive regulator of lipogenesis and also of fat storage, causing steatosis when upregulated [44]. In addition, the increase in *Gck* expression observed under a HFD, might provide the essential amount of NADPH to fuel lipogenesis [45]. The relatively higher levels than wild type of pAMPK and reduced upregulation of *Pparγ2* and *Gck* in livers of $Cat^{-/-}$ mice, which correlated with lower amount of *Fasn* and *Acc* mRNA are in accordance with reduced lipogenesis as the cause of limited steatosis after a HFD. Although there is not a clear mechanism by which alterations in the peroxisome could affect lipogenesis, products of peroxisomal lipolysis could represent either a significant amount of substrates for lipogenesis or PPARγ2 ligands [46]. Since liver steatosis upon feeding with a HFD can occur in the absence of peroxisomes and with decreased lipogenesis [47], indirect effects of lack of catalase on fatty acid transport and storage should also be considered (see below).

Fasting is another condition that promotes liver fat accumulation which, paradoxically, is associated with increased lipolysis and reduced lipogenesis [23]. A simple explanation to this phenomenon is the inability of liver to process all fatty acids released from the adipose tissue and imported into the liver under this condition; however, the actual mechanism is still a puzzle. Based on the regulation of gene expression, the reduced fat accumulation in the liver of mice lacking catalase upon fasting could hardly be due to the reduced expression levels of lipogenic genes before food deprivation, though it should not be discarded the possibility that a precondition (i.e., hormesis) is set in association to the reduced basal lipogenic activity under fed conditions. Increased lipolysis seems unlikely too, since not only minor differences were detected in levels of lipolytic gene expression, but also ketone bodies reached similar levels than wild type up to 48 h of fasting. Interestingly, NRF2, a transcription factor that controls an antioxidant response, prevents of excess fat accumulation in the liver upon fasting, apparently, by a mechanism that does not involve major alterations in lipogenesis or lipolysis [48,49]. It is tempting to speculate that increased β-oxidation due to fasting together with the lack of catalase elevates $H_2O_2$ to a level that does not cause significant oxidative damage and maintains NRF2 during fasting and, as a consequence, causes reduced fat accumulation. This mechanism could also contribute to reduced fat accumulation during a HFD, since lack of NRF2 promote hepatic steatosis. The regulation of *Pparγ* by NRF2 supports a role of this latter transcription factor in the liver metabolic phenotype of mice lacking catalase [50,51].

### 4.2. Lipid metabolism and aging

The effects of lack of catalase on liver fat accumulation point to lipid metabolism as the cause of shorter than wild type lifespan of $Cat^{-/-}$ mice. Accordingly, body weight and liver fat accumulation was reduced in aged $Cat^{-/-}$ mice. Although the cause of death of old animals has not been identified, this could be related to the mechanism that causes death of fasted mice. Survival of fasted mice is critically dependent on the existing energetic reserves at the time of food deprivation. In particular, after glycogen exhaustion in fasting conditions, fatty acid β-oxidation in the liver becomes essential for the production of ketone bodies, the systemic energetic source when glucose is scarce. Thus, survival of fasted newborn mice is compromised by the absence of ketolysis [26]. Newborn mice lacking catalase died upon fasting with a similar pattern as mice unable to use ketone bodies and, although the rapid use of ketone bodies limited the detection of their complete depletion before death, the decline in ketone bodies at 6 h of fasting were significant only in mice lacking catalase. In agreement with this view, adult $Cat^{-/-}$ mice that died under fasting correlated with an abrupt reduction in ketone bodies. Although we cannot discard that other reserves distinct from lipids also limit the survival of $Cat^{-/-}$ mice under fasting, our data suggest lipid shortage as a determinant of survival in conditions of food restriction or during aging. In agreement with this conclusion, the gene encoding PPARγ2, which promote lipid storage and its absence causes premature aging [52], was downregulated before fasting and in aged $Cat^{-/-}$ mice.

The participation of lipid metabolism in survival under food restriction and longevity has been previously determined. In *C. elegans*, DAF-16, a classical promotor of longevity in association with reduced insulin/IGF signaling, induces lipid synthesis [53]. However, the role of lipid metabolism in longevity is remarked by the increased lifespan of *C. elegans* lacking germ cells in which fat accumulation is an evident characteristic [54]. Interestingly, *SKN1*, a functionally-related *Nrf* homologous gene, is required for extended longevity in this condition, and although it protects against oxidative stress, also limits excess accumulation of fat [55]. Suggesting the participation of peroxisomal catalase in this phenomenon, *C. elegans* deficient in *ctl-3*, the gene encoding the peroxisomal catalase in this organism, exhibit, as in mice, shortened lifespan and reduced oxidative damage [56]. In addition, lack of peroxisomal catalase or $H_2O_2$ derived from fatty acid β-oxidation rescue *C. elegans* lacking AMPK from death under the hibernation-like dauer state by increasing, with minimal oxidative damage, accumulation of fat, an energetic reserve required for survival in this condition [57]. Therefore, the function of peroxisomal catalase in the regulation of lipid metabolism, maintenance of fat reserves, and longevity is conserved among distant organisms, though the mechanism may vary depending on environmental or genetic conditions.

### 4.3. Concluding remarks

The present work reveals a relevant role of catalase in the modulation of lipid metabolism. Physical interaction between lipid droplets and peroxisomes [12] suggests that peroxisomal activity and, thus, peroxisomal $H_2O_2$, are part of the regulatory mechanism. Since long fatty acids can be degraded in peroxisomes, this metabolic activity might explain why the penetrance of *Cat* deficiency in lipid metabolism was mainly revealed when mice ingested HFD or under extended

fasting. Genetic factors also appear to have a profound effect on the consequences associated with reduced catalase activity. For instance, an opposite phenotype to the one reported here (i.e., increased body weight and fat accumulation) has been observed in a mouse strain with in a slightly different genetic background (i.e., C57BL/6J vs. C57BL/6 N of the present study) [39,40]; the possible genetic modifier in this case is *Nnt*, a nuclear gene encoding the mitochondrial nicotinamide nucleotide transhydrogenase that is expected to affect the balance $NAD^+$/NADH and $NADP^+$/NADPH in mitochondria and has been related to body weight gain and obesity [58,59].

Catalase deficiency uncovers a mechanism by which ROS regulate lipid metabolism without oxidative damage, with implications in the mechanism that control longevity. Although alterations determined in the liver due to the lack of catalase are sufficient to provoke systemic metabolic alterations that can put at risk animal survival, direct cell autonomous damages in other tissue cannot be discarded. The ability of peroxisomal catalase to diminish cellular replicative senescence of human fibroblast [60] indicate that this enzyme can perform cell autonomous functions. However, the origin of the phenotype of animals lacking catalase cannot be conclusively attributed at this time to a cell autonomous function in hepatocytes, and non-cell autonomous functions involving, among others, adipose tissue should be considered.

The production and efficient use of reserves should be especially important for animals in the wild, since food is not equally available during the whole year. Thus animals, should have evolved mechanisms to survive under shortage of food, including those to store energetic resources and to efficiently use them [61]. Catalase can be an essential enzyme in these mechanisms that, through the control of peroxisomal $H_2O_2$, supports an optimal metabolic balance by regulating, at least, lipid metabolism. In this context, it is tempting to speculate that lifespan determination during evolution was critically influenced by the capacity of animals to survive under food restriction. The peroxisomal catalase could, then, be an evolutionary conserved component required for optimal use of metabolic reserves, before than protecting from the oxidative damage that characterizes aging.

## Acknowledgements

We appreciate the support by members of our group throughout fruitful discussions. We thank to all service units in our institution, in particular, the animal facility (supervised by Graciela Cabeza, Sergio Trujillo and Elizabeth Mata) and the DNA synthesis unit, without their assistance this work would not be possible. We also appreciate the technical contribution of Olivia Vázquez-Martínez, Deisy Gasca-Martínez and Mayra L. López-Cervantes of the INB-UNAM, and of Concepción Valencia of the IBT-UNAM. We also thank all the support provided by Landsteiner Scientific, SA de CV. This work was supported by grants IN209813 and IN213416 from PAPIIT-UNAM. JRPE was recipients of a CONACYT fellowship for graduate studies.

## Appendix A. Supplementary data

Supplementary data to this article can be found online at https://doi.org/10.1016/j.freeradbiomed.2019.02.016.

## References

[1] C. López-Otín, M.A. Blasco, L. Partridge, M. Serrano, G. Kroemer, The hallmarks of aging, Cell 153 (2013), https://doi.org/10.1016/j.cell.2013.05.039.
[2] J. a. Mattison, G.S. Roth, T.M. Beasley, E.M. Tilmont, A.M. Handy, R.L. Herbert, D.L. Longo, D.B. Allison, J.E. Young, M. Bryant, D. Barnard, W.F. Ward, W. Qi, D.K. Ingram, R. de Cabo, Impact of caloric restriction on health and survival in rhesus monkeys from the NIA study, Nature 489 (2012) 318–321, https://doi.org/10.1038/nature11432.
[3] J. Viña, C. Borras, K.M. Abdelaziz, R. Garcia-Valles, M.C. Gomez-Cabrera, The free radical theory of aging revisited: the cell signaling disruption theory of aging, Antioxidants Redox Signal. 19 (2013) 779–787, https://doi.org/10.1089/ars.2012.5111.
[4] T. Finkel, N.J. Holbrook, Oxidants, oxidative stress and the biology of ageing, Nature 408 (2000) 239–247, https://doi.org/10.1038/35041687.
[5] V.I. Pérez, A. Bokov, H. Van Remmen, J. Mele, Q. Ran, Y. Ikeno, A. Richardson, Is the oxidative stress theory of aging dead? Biochim. Biophys. Acta 1790 (2010) 1005–1014, https://doi.org/10.1016/j.bbagen.2009.06.003.Is.
[6] S. Imai, J. Yoshino, The importance of NAMPT/NAD/SIRT1 in the systemic regulation of metabolism and ageing, Diabetes Obes. Metab. 15 (2013) 26–33, https://doi.org/10.1111/dom.12171.
[7] L. Moldovan, N.I. Moldovan, Oxygen free radicals and redox biology of organelles, Histochem. Cell Biol. 122 (2004) 395–412, https://doi.org/10.1007/s00418-004-0676-y.
[8] M.P. Murphy, How mitochondria produce reactive oxygen species, Biochem. J. 417 (2009) 1–13, https://doi.org/10.1042/BJ20081386.
[9] G. Cozza, M. Rossetto, V. Bosello-Travain, M. Maiorino, A. Roveri, S. Toppo, M. Zaccarin, L. Zennaro, F. Ursini, Glutathione peroxidase 4-catalyzed reduction of lipid hydroperoxides in membranes: the polar head of membrane phospholipids binds the enzyme and addresses the fatty acid hydroperoxide group toward the redox center, Free Radic. Biol. Med. 112 (2017) 1–11, https://doi.org/10.1016/j.freeradbiomed.2017.07.010.
[10] K. Loh, H. Deng, A. Fukushima, X. Cai, B. Boivin, S. Galic, C. Bruce, B.J. Shields, B. Skiba, L.M. Ooms, N. Stepto, B. Wu, C.A. Mitchell, N.K. Tonks, M.J. Watt, M.A. Febbraio, P.J. Crack, S. Andrikopoulos, T. Tiganis, Reactive oxygen species enhance insulin sensitivity, Cell Metabol. 10 (2009) 260–272, https://doi.org/10.1016/j.cmet.2009.08.009.
[11] H.N. Kirkman, G.F. Gaetani, Mammalian catalase: a venerable enzyme with new mysteries, Trends Biochem. Sci. 32 (2007) 44–50, https://doi.org/10.1016/j.tibs.2006.11.003.
[12] I.J. Lodhi, C.F. Semenkovich, Peroxisomes: a nexus for lipid metabolism and cellular signaling, Cell Metabol. 19 (2014) 380–392, https://doi.org/10.1016/j.cmet.2014.01.002.
[13] M. Schrader, J. Costello, L.F. Godinho, M. Islinger, Peroxisome-mitochondria interplay and disease, J. Inherit. Metab. Dis. 38 (2015) 681–702, https://doi.org/10.1007/s10545-015-9819-7.
[14] J.M. Flynn, S. Melovn, SOD2 in mitochondrial dysfunction and neurodegeneration, Free Radic. Biol. Med. 62 (2013) 4–12, https://doi.org/10.1016/j.freeradbiomed.2013.05.027.
[15] R.S. Esworthy, R. Aranda, M.G. Martín, J.H. Doroshow, S.W. Binder, F.F. Chu, Mice with combined disruption of Gpx1 and Gpx2 genes have colitis, Am. J. Physiol. Gastrointest. Liver Physiol. 281 (2001) G848–G855.
[16] C. a Neumann, D.S. Krause, C.V. Carman, S. Das, D.P. Dubey, J.L. Abraham, R.T. Bronson, Y. Fujiwara, S.H. Orkin, R. a Van Etten, Essential role for the peroxiredoxin Prdx1 in erythrocyte antioxidant defence and tumour suppression, Nature 424 (2003) 561–565, https://doi.org/10.1038/nature01819.
[17] M.L. Sentman, M. Granström, H. Jakobson, A. Reaume, S. Basu, S.L. Marklund, Phenotypes of mice lacking extracellular superoxide dismutase and copper- and zinc-containing superoxide dismutase, J. Biol. Chem. 281 (2006) 6904–6909, https://doi.org/10.1074/jbc.M510764200.
[18] J.T. Haas, J. Miao, D. Chanda, Y. Wang, E. Zhao, M.E. Haas, M. Hirschey, B. Vaitheesvaran, R.V. Farese, I.J. Kurland, M. Graham, R. Crooke, F. Foufelle, S.B. Biddinger, Hepatic insulin signaling is required for obesity-dependent expression of SREBP-1c mRNA but not for feeding-dependent expression, Cell Metabol. 15 (2012) 873–884, https://doi.org/10.1016/j.cmet.2012.05.002.
[19] R. Radi, J.F. Turrens, L.Y. Chang, K.M. Bush, J.D. Crapo, B.A. Freeman, Detection of catalase in rat heart mitochondria, J. Biol. Chem. 266 (1991) 22028–22034.
[20] D. Luna-Moreno, O. Vázquez-Martínez, A. Báez-Ruiz, J. Ramírez, M. Díaz-Muñoz, Food restricted schedules promote differential lipoperoxidative activity in rat hepatic subcellular fractions, Comp. Biochem. Physiol. – A Mol. Integr. Physiol. 146 (2007) 632–643, https://doi.org/10.1016/j.cbpa.2006.02.039.
[21] C.C.J. Weydert, J.J. Cullen, Measurement of superoxide dismutase, catalase and glutathione peroxidase in cultured cells and tissue, Nat. Protoc. 5 (2009) 51–66, https://doi.org/10.1038/nprot.2009.197.
[22] Y.A. Moon, G. Liang, X. Xie, M. Frank-Kamenetsky, K. Fitzgerald, V. Koteliansky, M.S. Brown, J.L. Goldstein, J.D. Horton, The Scap/SREBP pathway is essential for developing diabetic fatty liver and carbohydrate-induced hypertriglyceridemia in animals, Cell Metabol. 15 (2012) 240–246, https://doi.org/10.1016/j.cmet.2011.12.017.
[23] J. Lee, J. Choi, S. Scafidi, M.J. Wolfgang, Hepatic fatty acid oxidation restrains systemic catabolism during starvation, Cell Rep. 16 (2016) 201–212, https://doi.org/10.1016/j.celrep.2016.05.062.
[24] T. Fukao, G.D. Lopaschuk, G.A. Mitchell, Pathways and control of ketone body metabolism: on the fringe of lipid biochemistry, Prostagl. Leukot. Essent. Fat. Acids 70 (2004) 243–251, https://doi.org/10.1016/j.plefa.2003.11.001.
[25] N. Mizushima, T. Yoshimori, B. Levine, Methods in mammalian autophagy research, Cell 140 (2010) 313–326, https://doi.org/10.1016/j.cell.2010.01.028.
[26] D.A. Cotter, David G. Avignon, A.E. Wentz, M.L. Weber, P.A. Crawford, Obligate role for ketone body oxidation in neonatal metabolic homeostasis, J. Biol. Chem. 286 (2011) 6902–6910, https://doi.org/10.1074/jbc.M110.192369.
[27] K.J. Lei, H. Chen, C.J. Pan, J.M. Ward, B. Mosinger, E.J. Lee, H. Westphal, B.C. Mansfield, J.Y. Chou, Glucose-6-phosphatase dependent substrate transport in the glycogen storage disease type-1a mouse, Nat. Genet. (1996), https://doi.org/10.1038/ng0696-203.
[28] J. Ezaki, N. Matsumoto, M. Takeda-Ezaki, M. Komatsu, K. Takahashi, Y. Hiraoka, H. Taka, T. Fujimura, K. Takehana, M. Yoshida, J. Iwata, I. Tanida, N. Furuya, D.M. Zheng, N. Tada, K. Tanaka, E. Kominami, T. Ueno, Liver autophagy contributes to the maintenance of blood glucose and amino acid levels, Autophagy 7 (2011) 727–736, https://doi.org/10.4161/auto.7.7.15371.

[29] K. Matsusue, M. Haluzik, G. Lambert, S.H. Yim, O. Gavrilova, J.M. Ward, B. Brewer, M.L. Reitman, F.J. Gonzalez, Liver-specific disruption of PPARγ in leptin-deficient mice improves fatty liver but aggravates diabetic phenotypes, J. Clin. Invest. 111 (2003) 737–747, https://doi.org/10.1172/JCI200317223.
[30] S. Tsukita, T. Yamada, K. Uno, K. Takahashi, K. Kaneko, Y. Ishigaki, J. Imai, Y. Hasegawa, S. Sawada, H. Ishihara, Y. Oka, H. Katagiri, Hepatic glucokinase modulates obesity predisposition by regulating BAT thermogenesis via neural signals, Cell Metabol. 16 (2012) 825–832, https://doi.org/10.1016/j.cmet.2012.11.006.
[31] Y.C. Long, J.R. Zierath, AMP-activated protein kinase signaling in metabolic regulation, J. Clin. Invest. 116 (2006) 1776–1783, https://doi.org/10.1172/JCI29044.1776.
[32] R.I. Fink, O.G. Kolterman, J. Griffin, J.M. Olefsky, Mechanisms of insulin resistance in aging, J. Clin. Invest. 71 (1983) 1523–1535 http://www.ncbi.nlm.nih.gov/pubmed/6345584.
[33] H. Zhang, Y. Li, Y. Fan, J. Wu, B. Zhao, Y. Guan, S. Chien, N. Wang, Klotho is a target gene of PPAR-γ, Kidney Int. 74 (2008) 732–739, https://doi.org/10.1038/ki.2008.244.
[34] M. Kuro-o, Y. Nabeshima, Y. Matsumura, H. Aizawa, H. Kawaguchi, T. Suga, T. Utsugi, Y. Ohyama, M. Kurabayashi, T. Kaname, E. Kume, H. Iwasaki, A. Iida, T. Shiraki-Iida, S. Nishikawa, R. Nagai, Mutation of the mouse *klotho* gene leads to a syndrome resembling ageing, Nature 390 (1997) 45–51, https://doi.org/10.1038/36285.
[35] Y. Xu, Z. Sun, Molecular basis of klotho: from gene to function in aging, Endocr. Rev. 36 (2015) 174–193, https://doi.org/10.1210/er.2013-1079.
[36] S.Y. Shi, Y.W. Lu, J. Richardson, X. Min, J. Weiszmann, W.G. Richards, Z. Wang, Z. Zhang, J. Zhang, Y. Li, A systematic dissection of sequence elements determining β-Klotho and FGF interaction and signaling, Sci. Rep. 8 (2018) 1–15, https://doi.org/10.1038/s41598-018-29396-5.
[37] L. Covarrubias, D. Hernández-García, D. Schnabel, E. Salas-Vidal, S. Castro-Obregón, Function of reactive oxygen species during animal development: passive or active? Dev. Biol. 320 (2008) 1–11, https://doi.org/10.1016/j.ydbio.2008.04.041.
[38] R.B. Hamanaka, A. Glasauer, P. Hoover, S. Yang, H. Blatt, A.R. Mullen, S. Getsios, C.J. Gottardi, R.J. DeBerardinis, R.M. Lavker, N.S. Chandel, Mitochondrial reactive oxygen species promote epidermal differentiation and hair follicle development, Sci. Signal. 6 (2013), https://doi.org/10.1126/scisignal.2003638 ra8-ra8.
[39] L. Piao, J. Choi, G. Kwon, H. Ha, Endogenous catalase delays high-fat diet-induced liver injury in mice, Korean J. Physiol. Pharmacol. 21 (2017) 317–325, https://doi.org/10.4196/kjpp.2017.21.3.317.
[40] C. Heit, S. Marshall, S. Singh, X. Yu, G. Charkoftaki, H. Zhao, D.J. Orlicky, K.S. Fritz, D.C. Thompson, V. Vasiliou, Catalase deletion promotes prediabetic phenotype in mice, Free Radic. Biol. Med. 103 (2017) 48–56, https://doi.org/10.1016/j.freeradbiomed.2016.12.011.
[41] O. Ivashchenko, P.P. Van Veldhoven, C. Brees, Y.-S. Ho, S.R. Terlecky, M. Fransen, Intraperoxisomal redox balance in mammalian cells: oxidative stress and interorganellar cross-talk, Mol. Biol. Cell 22 (2011) 1440–1451, https://doi.org/10.1091/mbc.E10-11-0919.
[42] Y.S. Ho, Y. Xiong, W. Ma, A. Spector, D.S. Ho, Mice lacking catalase develop normally but show differential sensitivity to oxidant tissue injury, J. Biol. Chem. 279 (2004) 32804–32812, https://doi.org/10.1074/jbc.M404800200.
[43] Y. Li, S. Xu, M.M. Mihaylova, B. Zheng, X. Hou, B. Jiang, O. Park, Z. Luo, E. Lefai, J.Y.J. Shyy, B. Gao, M. Wierzbicki, T.J. Verbeuren, R.J. Shaw, R.A. Cohen, M. Zang, AMPK phosphorylates and inhibits SREBP activity to attenuate hepatic steatosis and atherosclerosis in diet-induced insulin-resistant mice, Cell Metabol. 13 (2011) 376–388, https://doi.org/10.1016/j.cmet.2011.03.009.
[44] M. Bedoucha, E. Atzpodien, U.A. Boelsterli, Diabetic KKAy mice exhibit increased hepatic PPARγ1 gene expression and develop hepatic steatosis upon chronic treatment with antidiabetic thiazolidinediones, J. Hepatol. 35 (2001) 17–23, https://doi.org/10.1016/S0168-8278(01)00066-6.
[45] E.S. Jin, M.H. Lee, R.E. Murphy, C.R. Malloy, Pentose phosphate pathway activity parallels lipogenesis but not antioxidant processes in rat liver, Am. J. Physiol. Metab. 314 (2018) E543–E551, https://doi.org/10.1152/ajpendo.00342.2017.
[46] I.J. Lodhi, L. Yin, A.P.L. Jensen-Urstad, K. Funai, T. Coleman, J.H. Baird, M.K. El Ramahi, B. Razani, H. Song, F. Fu-Hsu, J. Turk, C.F. Semenkovich, Inhibiting adipose tissue lipogenesis reprograms thermogenesis and PPARγ activation to decrease diet-induced obesity, Cell Metabol. 16 (2012) 189–201, https://doi.org/10.1016/j.cmet.2012.06.013.
[47] H. Weng, X. Ji, Y. Naito, K. Endo, X. Ma, R. Takahashi, C. Shen, G. Hirokawa, Y. Fukushima, N. Iwai, Pex11 deficiency impairs peroxisome elongation and division and contributes to nonalcoholic fatty liver in mice, AJP Endocrinol. Metab. 304 (2013) E187–E196, https://doi.org/10.1152/ajpendo.00425.2012.
[48] Y. Li, X. Chao, L. Yang, Q. Lu, T. Li, W.X. Ding, H.M. Ni, Impaired fasting-induced adaptive lipid droplet biogenesis in liver-specific Atg5-deficient mouse liver is mediated by persistent nuclear factor-like 2 activation, Am. J. Pathol. 188 (2018) 1833–1846, https://doi.org/10.1016/j.ajpath.2018.04.015.
[49] J. Paek, J.Y. Lo, S.D. Narasimhan, T.N. Nguyen, K. Glover-Cutter, S. Robida-Stubbs, T. Suzuki, M. Yamamoto, T.K. Blackwell, S.P. Curran, Mitochondrial SKN-1/Nrf mediates a conserved starvation response, Cell Metabol. 16 (2012) 526–537, https://doi.org/10.1016/j.cmet.2012.09.007.
[50] V.R. More, J. Xu, P.C. Shimpi, C. Belgrave, J.P. Luyendyk, M. Yamamoto, A.L. Slitt, Keap1 knockdown increases markers of metabolic syndrome after long-term high fat diet feeding, Free Radic. Biol. Med. 61 (2013) 85–94, https://doi.org/10.1016/j.freeradbiomed.2013.03.007.
[51] Y. Tanaka, L.M. Aleksunes, R.L. Yeager, M. a Gyamfi, N. Esterly, G.L. Guo, C.D. Klaassen, NF-E2-Related factor 2 inhibits lipid accumulation and oxidative stress in mice fed a high-fat diet, J. Pharmacol. Exp. Therapeut. 325 (2008) 655–664, https://doi.org/10.1124/jpet.107.135822.
[52] C. Argmann, R. Dobrin, S. Heikkinen, A. Auburtin, L. Pouilly, T.A. Cock, H. Koutnikova, J. Zhu, E.E. Schadt, J. Auwerx, Pparγ2 is a key driver of longevity in the mouse, PLoS Genet. 5 (2009), https://doi.org/10.1371/journal.pgen.1000752.
[53] M. McCormick, K. Chen, P. Ramaswamy, C. Kenyon, New genes that extend Caenorhabditis elegans' lifespan in response to reproductive signals, Aging Cell 11 (2012) 192–202, https://doi.org/10.1111/j.1474-9726.2011.00768.x.
[54] C. Longevity, M.C. Wang, E.J.O. Rourke, G. Ruvkun, Fat metabolism links germline stem, Science (80) 322 (2008) 957–960.
[55] M.J. Steinbaugh, S.D. Narasimhan, S. Robida-Stubbs, L.E. Moronetti Mazzeo, J.M. Dreyfuss, J.M. Hourihan, P. Raghavan, T.N. Operaña, R. Esmaillie, T.K. Blackwell, Lipid-mediated regulation of SKN-1/Nrf in response to germ cell absence, Elife 4 (2015) 1–30, https://doi.org/10.7554/eLife.07836.
[56] O.I. Petriv, R.A. Rachubinski, Lack of peroxisomal catalase causes a progeric phenotype in Caenorhabditis elegans, J. Biol. Chem. 279 (2004) 19996–20001, https://doi.org/10.1074/jbc.M400207200.
[57] M. Xie, R. Roy, Increased levels of hydrogen peroxide induce a HIF-1-dependent modification of lipid metabolism in AMPK compromised C. elegans dauer larvae, Cell Metabol. 16 (2012) 322–335, https://doi.org/10.1016/j.cmet.2012.07.016.
[58] A. Nicholson, P.C. Reifsnyder, R. Malcolm, C. a Lucas, R. Grant, W. Zhang, E.H. Leiter, B. Harbor, Diet induced obesity in two C57BL/6 substrains with intact or mutant Nicotinamide Nucleotide Transhydrogenase (Nnt) gene, Obesity 18 (2011) 1902–1905, https://doi.org/10.1038/oby.2009.477.Diet.
[59] J.A. Ronchi, T.R. Figueira, F.G. Ravagnani, H.C.F. Oliveira, A.E. Vercesi, R.F. Castilho, A spontaneous mutation in the nicotinamide nucleotide transhydrogenase gene of C57BL/6J mice results in mitochondrial redox abnormalities, Free Radic. Biol. Med. 63 (2013) 446–456, https://doi.org/10.1016/j.freeradbiomed.2013.05.049.
[60] J.E. Legakis, Peroxisome senescence in human fibroblasts, Mol. Biol. Cell 13 (2002) 4243–4255, https://doi.org/10.1091/mbc.E02-06-0322.
[61] J.A. Viscarra, R.M. Ortiz, Cellular mechanisms regulating fuel metabolism in mammals: role of adipose tissue and lipids during prolonged food deprivation, Metabolism 62 (2013) 889–897, https://doi.org/10.1016/j.metabol.2012.12.014.